Int. J. Cancer: **123,** 2105–2112 (2008)

Multiple pathways for Epstein-Barr virus episome loss from nasopharyngeal carcinoma

Dirk P. Dittmer[1]*, Chelsey J. Hilscher[1], Margaret L. Gulley[2], Eric V. Yang[3], Min Chen[3] and Ronald Glaser[3,4]

[1]*Lineberger Comprehensive Cancer Center, Center for AIDS Research and Department of Microbiology and Immunology, University of North Carolina, Chapel Hill, NC*
[2]*Department of Pathology and Laboratory Medicine, University of North Carolina, Chapel Hill, NC*
[3]*Institute for Behavioral Medicine Research, The Ohio State University Medical Center, Columbus, OH*
[4]*Department of Molecular Virology, Immunology and Medical Genetics, Comprehensive Cancer Center, Columbus, OH*

Epstein-Barr virus (EBV) is the prototypical example for episomal persistence of genetic information. Yet, little is known about how this viral episome is lost. Episome loss occurs naturally in nasopharyngeal carcinoma (NPC) upon explantation into culture. Using whole-genome profiling, we found evidence for 2 different pathways of episome loss: (*i*) rapid loss of the entire episome or (*ii*) successive mutation/deletion of the episome until at least 1 essential cis-element is destroyed. This second phenotype was seen in a clone of HONE-1 NPC cells that maintains the EBV episome for prolonged time in culture. The conceptual insights provided by our quantitative analysis should aid our understanding of mammalian episomes, as well as lead to designs to cure latent viral infection.

Key words: episome; real-time QPCR; Epstein-Barr virus; nasopharyngeal carcinoma; epithelial cells

Epstein-Barr virus (EBV) is a human oncogenic virus, which has been associated with infectious mononucleosis (IM),[1] African Burkitt's lymphoma (BL)[2] and nasopharyngeal carcinoma (NPC).[3] In these cancers, the virus is maintained extrachromosomally as a circular episome. The EBV latent origin of replication (ori-P), the EBV nuclear antigen 1 (EBNA-1) coding region and the promoter are the only cis-elements required to maintain the latent episome (or any artificial circular plasmid).[4–6] Only the Qp promoter is used to maintain EBNA-1 expression in NPC.[7]

In EBV-positive NPC, every tumor cell contains the viral episome. In contrast to lymphocyte lineage tumors, it has been exceedingly difficult to establish permanent cell lines from NPC tumors that maintain the EBV episome during continuous culture. Rare examples of such cell lines include CNE-1 and CNE-2, which were derived from NPC patients in China (Cancer Institute, Beijing, 1978)[8] and NPC/HK1 from a patient in Hong Kong.[9] Even though these cell lines were obtained from EBV genome positive NPC biopsies, none remained EBV genome positive after prolonged culture. Upon experimental infection of epithelial cells in culture, the EBV viral genome is rapidly lost, unless drug selection is applied.[10] Other EBV-positive epithelial-lineage primary tumor cells, such as HNE-1, also rapidly lose the virus upon explantation into culture. This has severely hampered our understanding of EBV-associated epithelial lineage tumors such as NPC and EBV-positive gastric carcinomas.

Our laboratory, in collaboration with Dr. Kaitai Yao and his group at the Hunan Medical University (Hunan, People's Republic of China) were able to establish an NPC-derived cell line that contained the EBV genome in a stable manner with the cell genome.[11] This cell line, HONE-1 clone 40, was characterized in previous reports.[11–13] As far as we know, this was the first NPC cell line to contain a stable EBV genome for over 40 passages. Unfortunately, this cell line is no longer available. Here, we used another clone that was isolated from the same NPC biopsy, HONE-1 clone 13 cells. HONE-1 clone 13 cells were EBV DNA positive at early passage, but the relationship between EBV DNA and the NPC tumor cells was unstable. This resembles the prototypical response of EBV-infected epithelial cell tumors after explantation into culture. We have taken advantage of this model to explore the fundamental mechanisms of EBV episome loss.

Whole EBV genome profiling shows that in addition to losing the entire viral episome at once, as previously observed,[5] NPC cells can also lose the episome through accumulative mutations, deletions and recombination. The rate of loss by this second, novel mechanism is slower. Since HONE-1 clone 13 cells do not depend on EBV for growth in culture, defective genomes can accumulate. This second, gradual mechanism of episomal loss may explain the variation found in EBV episome maintenance in current NPC models.

Material and methods

Tissue culture

In this study, we used "uncloned", parental HONE-1 cells and HONE-1 clone 13 cells. Both cell lines were isolated from the same NPC biopsy as the HONE-1 clone 40 cells. Every effort had been made to prepare all HONE-1 clones as quickly as possible as the parental HONE-1 cells were grown out from the NPC tumor specimen. All cultures were maintained at 37°C and grown in RPMI 1640 medium supplemented with 10% fetal bovine serum (FBS) as described.[14]

DNA extraction

Cells were trypsinized, pelleted at 1,700 rpm for 5 min in a tissue culture centrifuge, and washed twice with calcium and magnesium-free phosphate-buffered saline. Total DNA from 1×10^6 cells was extracted by proteinase K digestion (at 1 mg/ml) in 100 μl hypotonic lysis buffer (10 mM Tris/HCl pH 8.0, 2.5 mM $MgCl_2$, 1% IGEPAL, 1% Tween-20) for 30 min at 50°C in a PCR tube. Subsequently, proteinase K was inactivated by incubation at 95°C for 15 min. Lysates were divided into 10-μl aliquots and stored at −80°C until use.

Primer design

Primers were designed using the PrimeTime program,[15] which is based on the European Molecular Biology Open Software Suite (EMBOSS)[16] and ePrimer3[17] using the EBV genome as input sequence (nucleotide entry GI:23893576).

Additional Supporting Information may be found in the online version of this article.

Grant sponsor: The Ohio State University Comprehensive Cancer Center core grant; Grant sponsor: NCI; Grant number: CA16058; Grant sponsor: Gilbert and Kathryn Mitchell Endowment; Grant numbers: CA109232, DE018304.

***Correspondence to:** Lineberger Comprehensive Cancer Center, Center for AIDS research and Department of Microbiology and Immunology, & Department of Pathology and Laboratory Medicine, University of North Carolina, Chapel Hill NC 27599, USA. E-mail: ddittmer@med.unc.edu

Received 22 May 2007; Revised 26 September 2007; Accepted after revision 20 March 2008
DOI 10.1002/ijc.23685
Published online 7 August 2008 in Wiley InterScience (www.interscience.wiley.com).

Real-time QPCR

Real-time QPCR for EBV latent membrane protein-1 (LMP-1), GAPDH and all other EBV gene loci DNA was performed as described[18,19] using SYBR Green as the method of detection. Primer sequences are provided in Supplemental Table I. EBV nuclear antigen 1 (EBNA-1) and the gene for the ribosomal 18S RNA were quantified using TaqMan™. Briefly, DNA was diluted with distilled H_2O to yield 250 μl, mixed with 500 μl 2× SYBR PCR mix (Applied Biosystems), and aliquoted into individual wells (12.5 μl/well) of a 96-well PCR plate using a CAS-1200 robot (Corbett). Individual EBV primers were used at 267 nM final concentration. Real-time quantitative PCR was performed on an MJR Opticon2 cycler (see Ref. 20 for details). The cycle-threshold values (CT) were determined by automated analysis. Lower CT values correspond to higher gene copy number. The threshold was set to 5 times the standard deviation (SD) of the nontemplate control (NTC).

Statistical analysis

Calculations were performed using Excel™ (Microsoft, Redwood, WA) and SPSS™ v11.0 (SPSS Science, Chicago, IL) under Macintosh OS v.10.4. Additional calculations were performed in Maple™ v.10 (Waterloo Software). Hierarchical clustering was performed using ArrayMiner™ software (Optimal Design, Brussels, Belgium) as previously described.[21]

Chromosome analysis, mitochondrial DNA analysis and EBER in situ hybridization

Exponentially growing HONE-1 parental and HONE-1 clone 13 cells were fixed using standard laboratory procedures. Cell suspensions were prepared and dropped onto precleaned, warm, wet slides. The slides were aged at 90° C for 1 hr, banded with trypsin and stained with Wright stain. Banded metaphases were analyzed using a Zeiss Axioskop 40 microscope. For each cell line metaphases were karyogramed using an Applied Imaging Karyotyping System. The metaphases were described using ISCN (2005).[22]

Using primers specific for the human mitochondrial region, which are validated for forensic PCR,[23] we PCR-amplified 2 regions from every passage of cells used in our experiments and sequenced the resulting PCR products. Sequences were aligned using Sequencher v4.8 (Gene Codes Corporation, Ann Arbor, MI).

For EBER-ISH, pellets were enmeshed in thrombin using a Cytoblock Kit and fixed in 10% Formalin overnight followed by paraffin embedding and cutting of 5-μm thick sections. H&E staining confirmed presence of cells. *In situ* hybridization was carried out on a Ventana Benchmark instrument using an EBER probe (Ventana Medical System, probe CAT#780-2842). Parallel hybridization with an oligodT probe (Control probe CAT# 780-2846) showed the extent to which RNA was preserved and available for hybridization. A nasopharyngeal carcinoma biopsy section used as a control showed sensitive and specific EBER staining. ISH results were evaluated for staining intensity (0–4+) and proportion (0–100% of cells).

Mathematical model

Our data result from QPCR amplification with multiple primer pairs $p_{1\ldots n}$, $n = 1, \ldots, 75$ each located within an EBV orf. We have total DNA from several successive passages 0, 4, 8 and 22 indicated by t_k, $k = 1\ldots4$. To exclude variation due to DNA extraction efficiency and cell number per flask, raw EBV CT values were normalized to a single host DNA-specific primer to yield $dCT = CT_{EBV\ primer\ 1\ldots75} - CT_{gapdh}$. Under the hypothesis of whole chromosome loss, the differences between any 2 primers pairs $ddCT = dCT_i - dCT_j$ remained constant for different passages t_k. They reflect the ratio of the relative primer efficiencies K_{eff}. The ddCT are normal distributed.

To approximate recombination rates for circular episomes, Figure 5 tests the hypothesis that any 2 adjacent orfs i and $i + 1$ are either retained or lost together. The more distant any 2 orfs are from each other, such as orf i and orf $i + 2$, or orf i and orf $i + 3$, and so on, the more recombination can be expected. One orf may be lost and the other retained during continuous culture. This is calculated by comparing $ddCT_{i,i+1} = dCT(p_i) - dCT(p_{i+1})$ to $ddCT_{i,i+2} = dCT(p_i) - dCT(_{i+2})$ for all primers at a given passage t_k. Between passages t we expect a higher correlation of $i + 1$ differences to each other than to $i + 2$ differences.

Results

EBV DNA is lost upon explantation of NPC tumor cells at different rates

In the absence of selection, EBV-infected epithelial cells lose the virus over time. This represents a major technical limitation to experimental EBV virology, which has plagued the establishment of EBV-positive adherent cell lines and slowed investigations into EBV-associated epithelial cell cancers. Yet, it resembles the natural course of events after explantation of EBV-positive tumor cells from EBV-associated epithelial cancers, such as NPC, and provides a general model system to study large (≥100 kbp) episome loss from mammalian cells.

Here, we employ the HONE-1 cell system to understand the mechanism of the loss of EBV episomal DNA in NPC tumor cells. Previously, viral load was measured using a single probe directed against a short segment of the episome by either DNA hybridization or PCR. These studies showed that the EBV episome was lost upon the adaptation of primary NPC tumor cells to growth in an artificial medium.[24,25] The experimental design using only a single probe for the viral genome could not determine whether the viral episome was being lost in 1 piece or whether it was being lost through cumulative deletions. This could theoretically be accomplished by successive subgenomic deletions first leading to defective genomes, which are then lost only after an essential gene function becomes impaired. To decide between these 2 scenarios, we use a real-time QPCR-based EBV genome array that contains 1 primer pair for each viral orf.

Cells from cultures of HONE-1 parental and HONE-1 clone 13 cells were completely karyogramed. Supplemental Figures 1a and 1b show karyotypes of the 2 HONE-1 cell lines. The 2 NPC cell lines were almost identical, near-tetraploid, with nearly all of the same structural abnormalities, including the same marker chromosomes. The only difference between the HONE-1 cell lines were the presence of 3 normal 16s in the parental cell line and 4 normal 16s in HONE-1 clone 13 cells, in the parental cell line, which was not seen in HONE-1 clone 13 cells and a twelfth marker in HONE-1 clone 13 cells not seen in the parental cell line. Both cell lines showed some cell-to-cell heterogeneity. Complete ISCN descriptions are shown in Supplemental Table II.

To confirm prior reports on HONE-1 cells, we used samples previously prepared from cells frozen at different passage levels. Our definition of a passage indicates the number of times the cells were trypzinized and seeded into new flasks. We extracted DNA and conducted PCR using primer pairs directed against 2 different EBV genes (LMP-1 and EBNA-1). To determine whether the HONE-1 cells contained the EBV genome, we performed PCR with primers specific for LMP-1. Primers directed against GAPDH were used as control for DNA purification. In this and subsequent experiments only a single band was observed after PCR analysis attesting to the specificity of all primers (Fig. 1*a* and data not shown). Two independent cultures of parental HONE-1 cells at Passage 8 contained EBV DNA, whereas in 2 later passages, 12 and 21, the amount of the EBV DNA was below the detection limit of the assay. Based on EBER-ISH, 2% of cells were EBV positive at Passage 9 (data not shown). Of note, even though late passage parental HONE-1 and HONE-1 clone 13 no longer contain the EBV genome or any pieces of it (see later), the cells continue to grow in culture indefinitely and also are tumorigenic

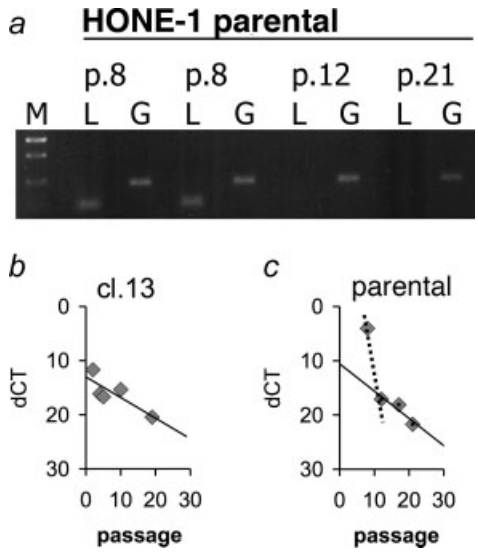

FIGURE 1 – (*a*) Ethidium bromide stained 2% agarose gel of the products of real-time QPCR using primers specific for GAPDH (labeled G) or EBV Lmp-1 (labeled L). The input was DNA from Hone-1 parental cells at Passage 8 (labeled p.8) from duplicate cultures, Passage 12 (labeled p.12) and Passage 21 (labeled p.21). Molecular weight markers (M) are indicated on the left. (*b*, *c*) Shown on the vertical axis is the relative abundance of EBV DNA (dCT) on a log scale. Higher CT corresponds to lower abundance. The real-time QPCR result for EBV DNA was normalized to total DNA to yield the average copy number per cell. The limit of detection was dCT = 25, which corresponds to less than 1 copy per million cells. The horizontal axis shows the passage number for either cl.13 or the primary HONE-1 cell explant culture.

in nude mice (unpublished observation). This result corroborates the known phenotype of EBV episome loss in NPC explants.

Using primers specific for the human mitochondrial region, which were validated for forensic PCR, we amplified 2 regions of the mitochondrial genome from every passage of cells used in our experiments, sequenced the resulting PCR products and looked for evidence of single nucleotide sequence polymorphism (SNP) (Supplemental Table III). There were no SNPs in Region 1. Region 2 showed 9 SNPs, which were the result of a double peek in 1 sample, namely clone 13 Passage 2. All other sequences were identical. This demonstrates that all the cells analyzed herein represent clonal populations that stemmed from the same donor.

Evidence for biphasic EBV episomal loss from primary NPC explant cultures

We improved upon prior studies by using real-time QPCR with primers directed against the EBNA1 coding region. This determined the total rate of episome loss, since EBNA1 is required for latent oriP-dependent replication and partitioning. Any cell that does not express EBNA-1 loses all EBV episomes, whereas even minimal EBV episomes are maintained as long as EBNA-1 protein is present. Similar overall DNA amounts were used as input. This was evidenced by measuring the amount of the cellular gene for 18S ribosomal RNA, which yielded a mean CT_{18S} of 19.81 with a SD of 1.92. The 95% confidence interval (^{95}CI) was 18.96–20.69 across $n = 20$ samples. CT values generated from real-time QPCR represent a logarithmic measure of target copy number, wherein a lower CT value represents a higher level of target. A SD of 1.92 corresponds to $2^{1.94} = 3.7$-fold. To adjust for variability in DNA input levels, we normalized CT values for EBNA-1 (CT_{EBNA1}) to host DNA as follows: $dCT = CT_{EBNA1} - CT_{18S}$ (Figs. 1*b* and 1*c*). All reactions were conducted in duplicate. Technical replicates, which reflect the overall pipetting and detection error, differed on average by 0.89 CT units (^{95}CI: 0.00–1.77, $n = 10$) for CT_{18S}. The reproducibility of duplicates was not affected by input DNA levels. This can be shown by a lack of correlation between variability and mean levels.[26] The regression coefficient r^2 of difference *vs*. mean was 0.0338, demonstrating that we operated within the linear range of the assay. To obtain biological replicates, we determined the DNA content for HONE-1 clone 13 cells at Passage 4 and immediately thereafter at Passage 5. This yielded identical results for viral DNA levels ($dCT_{passage\ 4} = 16.12$ and $dCT_{passage\ 5} = 16.67$, respectively, Fig. 1*b*) and attests to the reproducibility of our DNA extraction procedure.

We used cells of 2 different NPC cultures. HONE-1 clone 13 is a unique clonal derivative of the original HONE-1 explant culture. It has been shown to retain the EBV genome in the absence of selection at early passages and without rapid loss of the EBV genome for some time.[11,12] It shows a constant, slow rate of EBV genome loss (Fig. 1*b*), which correlates linearly with passage number ($r^2 = 0.688$ with slope of $m = 0.38 \pm 0.15$, $n = 5$). By contrast, the uncloned HONE-1 cell population, representing the parental explant population, showed a biphasic rate of episomal loss (Fig. 1*c*): first, a typical, rapid phase of EBV episomal loss (as previously observed[27]), followed by a "slow", more gradual rate of loss, which correlates linearly with passage number ($r^2 = 0.865$ with a slope of $m = 0.50 \pm 0.20$, $n = 3$). The rate of episome loss in the latter phase of parental HONE-1 cells was not significantly different from the rate of loss of HONE-1 clone13 cells. After Passage 21, the EBV DNA signal was below the limit of detection in both cultures. The biphasic behavior of the uncloned HONE-1 population is typical for primary NPC explant cultures and was our first indication of 2 pathways for EBV episome loss: the first, rapid and almost catastrophic; the second, gradual and correlated with passage number in culture.

We hypothesized that the 2 quantitative different phases of episome loss correspond to 2 qualitatively different mechanisms of episome loss and that catastrophic loss precedes gradual degradation. The parental, uncloned cell population starts out with a higher average EBV copy number as reflected in a lower dCT_{18S} at Passage 8. This is followed by rapid episome loss as reflected in an increased dCT_{18S} at later passages (Fig. 1*c*). At around Passage 10 both HONE-1 clone 13 and parental cell populations exhibit equivalent average copy numbers, and from that point on changed at a similar rate.

These data support the idea of a finite carrying capacity for long-term episomal maintenance in latently infected cells. Although clonal variation can result in initial high variability of episome copy number (Passage < 10), once the cells become culture-adapted (Passage > 10) both NPC cultures carry the same average EBV episome number and lose the episome at a similar constant rate. We do not know the molecular mechanism behind this phenotype. One could speculate, however, that a host factor, such as a replication licensing protein, becomes rate limiting as the cells adapt from the tumor microenvironment to single cell growth in culture.

Different pathways can account for loss of episomes

We envision 2 scenarios, depicted in Figure 3, to explain the loss of EBV episomes: (*i*) the entire episome is either propagated to the next generation or lost as a whole; (*ii*) intraepisomal mutation, deletion and/or recombination takes place generating 2 partial episomes. Only the part of the genome that contains all essential cis-elements is propagated to the next generation. These scenarios are not mutually exclusive.

These scenarios lead to different genome configurations over time, which we measured by quantifying the level of all different EBV genes (primer pairs $p_{1 \ldots n}$, $n = 75$), each located within a different EBV orf in relation to each other. Each of these loci was quantified independently using real-time QPCR at Passages 0, 4, 8, 22 after explantation from the tumor.

If the entire episome is lost as a whole (Figure 2*a*), then all orfs are lost at the same rate. At each passage, each orf will be present

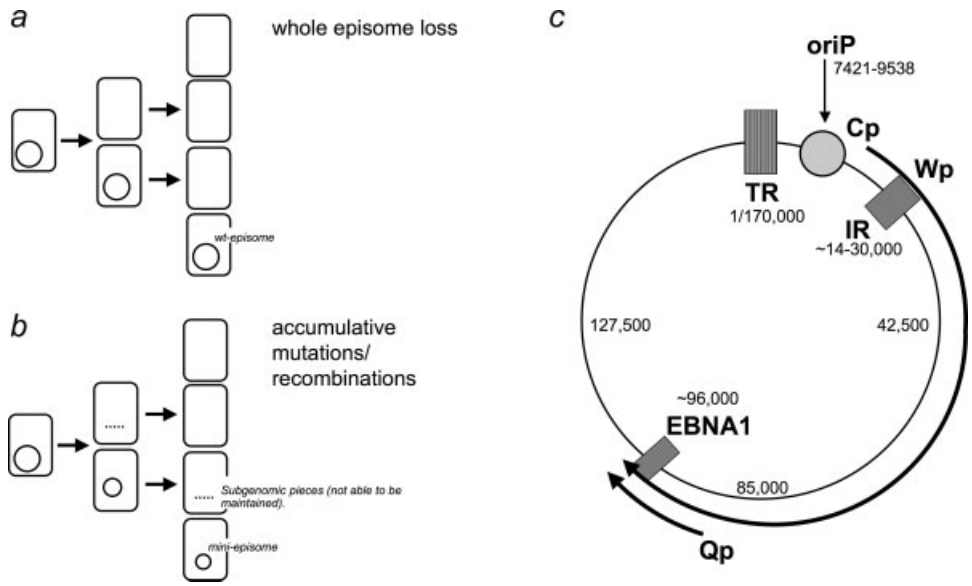

FIGURE 2 – Possible scenarios for EBV episomal loss: (*a*) Loss of the entire episome at once (all markers) and (*b*) progressive loss of nonessential regions (adjacent markers) by successive recombination events. Any cell that does not retain EBNA1, oriP and Qp loses all EBV genome DNA at the next cell division. (*c*) Relative positions of the essential elements for EBV latent persistence in NPC (Type II).

at the same copy number within the culture. Alternatively, if the episome shrinks by recombining out nonessential orfs (Fig. 2*b*), individual orfs will be lost at different rates. At each passage a given orf may or may not be present at the same copy number as all other orfs. The further any 2 orfs are apart from each other, the more likely a recombination event can occur. If EBNA, oriP and Qp were in the same location, the chance of losing a particular orf by recombination would increase linearly as its distance increases from the oriP. In EBV, however, the 3 essential elements EBNA, oriP and Qp are located in different places on the circular episome. Therefore, a linear distance relationship is not expected (Fig. 2*c*). The recombination distance function for circular episomes with multiple essential elements is not trivial and was approximated as described in the Material and methods section.

An important aspect of this model is that the pattern of orf loss relative to each other is not affected if the episome replicates in between host cell divisions[28] or if not. Traditionally, the rate of single gene loss is calculated by normalizing the levels for each single orf (as measured by a real-time QPCR primer pair p_i) at each passage to cellular DNA (18S RNA gene locus) $dCT(p_i) = CT(p_i) - CT_{18s}$ and plotting $dCT(p_i)$ against passage number as in Figure 1. This assumed rate of loss to be constant. In contrast, in our novel array approach, we normalize CT for each primer p_i at each passage t_k to the median of all 75 primers for that sample $dCT(p_i) = CT(p_i) - CT(p_{median})$. This yields the relative copy number of 1 orf to all others. If an orf is recombined out or lost by deletion, its relative copy number will decrease. This is reflected by an increased $dCT(p_i)$ value, as more cycles are needed to detect residual cells within the flask that still carry an intact episome. Importantly, this normalization method neither requires that the rate of viral episome loss be constant nor that all primers have equivalent efficiency.[15,29]

Our model further assumes that any fragment that is separated from the oriP is irretrievably lost, and that any time a recombination/cell division event separates EBNA-1, oriP and Qp, all viral genome fragments are lost during subsequent cell division, *i.e.*, there is only 1 latent origin per genome.

Of note, at each passage only a fraction of cells is transferred to the next flask, such as only 10% in a "1:10 split". This explains why pieces of EBV, which are not able to replicate in between passages, become diluted out with increasing passage number. The only exception here would be pieces that were integrated into the host chromosome genome. Since both NPC cultures lost all EBV genes at the last passage, we conclude that this was not the case.

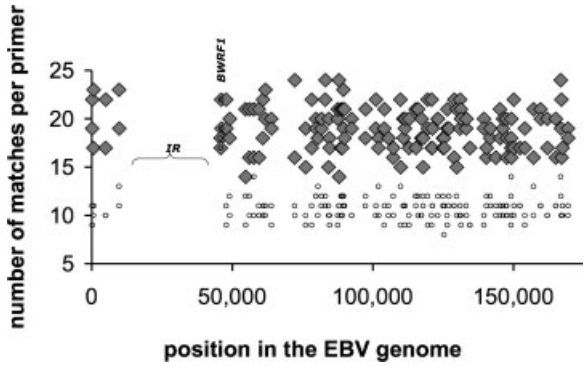

FIGURE 3 – Genome coverage with 75 EBV orf-specific primer pairs. Plotted is the number of matches for a given primer on the vertical axis *vs.* the position of the primer on the horizontal axis. Primers used are shown in gray diamonds. Here, the number of matches equals the total primer length. The next best match for each primer on the EBV genome is shown in open circles. Numbers indicate approximate map positions in bp.

A real-time QPCR array for EBV allows comparative gene copy number determination

We used our real-time QPCR-based microarray for EBV[18,19] to experimentally distinguish between the 2 possible scenarios. Figure 3 shows the distribution of primers across the EBV genome. The actual primers used in the array (gray diamonds) show 100% sequence identity. Therefore, the number of matches is equal to the total primer length. Using blastN we also computed the next best match for each primer on the EBV genome, which could result in missprimed amplification products. The next best match for each primer on the EBV genome is shown in open circles. There are at least seven [^{95}CI: 7.82, . . . , 8.53 (n = 160)] nucleotide mismatches between the correct match (gray diamonds) and the next best match (open circles) making it unlikely that under

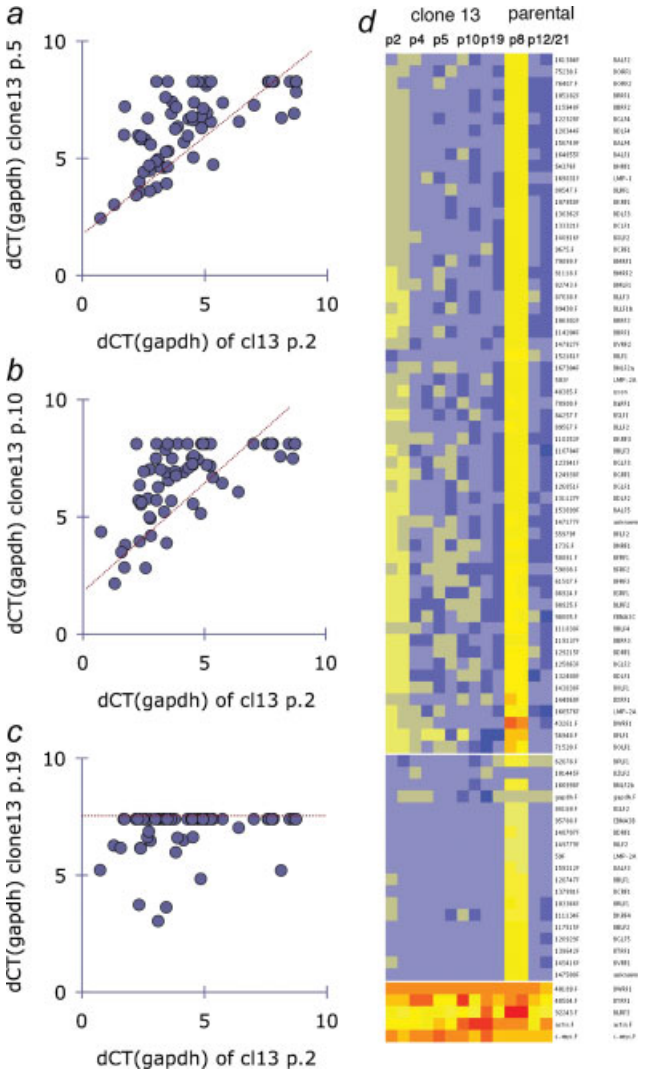

FIGURE 4 – (*a–c*) Plot of log relative levels (dCT(GAPDH)) for HONE-1 clone 13 cells passage 5, 10 and 19 on the vertical and Passage 2 on the horizontal axis. Shown is the mean of biological duplicates. (*d*) Tree-view representation of all CT data. Yellow indicates higher and blue lower levels. We used median-centered CT values without removing outliers as basis for clustering.

our QPCR conditions (T_m = 62°, extension time 60 sec) a given primer would anneal anywhere else but at its cognate site. Exceptions were the BWRF1 primers, which can anneal at multiple locations in the BWRF1 repeats. Except for the internal repeat (IR) region, our array covers the entire genome evenly. The mean distance between adjacent primers was 1714 bp (^{95}CI: 1394,..., 2033 bp for n = 75 primers pairs). Hence, this array has a resolution of ~2,000 bp.

We used this genome array to determine EBV genome copy number (Fig. 4). All HONE-1 clone 13 cell time points (Passages 2, 4, 5, 10, 19) were measured in biological duplicates, HONE-1 parental cells at time point Passage 8 were measured in biological duplicate, and Passages 12 and 21 represent single measurements. All measurements were normalized to total DNA using primers specific for GAPDH. Figure 4 plots dCT_{gapdh} for each EBV orf in HONE-1 clone 13 cells at successive passages[5,10,19] on the vertical axis relative to dCT_{gapdh} for each EBV orf at Passage 2 on the horizontal axis.

With increasing passage number most EBV-derived signals were lost, as evidenced by an increase in dCT. Because 40 was the maximal cycle number in our QPCR protocol, the maximum value of dCT was 40-CT_{gapdh}, which is ~8 units. At Passage 5 (Fig. 4*a*), we were able to detect almost all orfs. Except for a few outliers relative abundance (dCT) correlated linearly with the abundance at Passage 2 as indicated by the red regression line. At Passage 10 (Fig. 4*b*), many orfs were no longer detectable as indicated by increased dCT. At Passage 19 (Fig. 4*c*), only orfs corresponding to genome positions 584 and 166807 (LMP2A), 147521, 161974 (BALF2), 149133 (BVRF2), 143664 (BXLF1), 133162 (BDLF1), 111336 (BKRF4), 89805,89476 (BLLF2, BLLF1b), 87423, 84523 (BSLF1, BSRF1), 79673 (BaRF1), 72113 (BOLF1), 63798 (BPLF1), 57556 (BFLF1), 9672 (BCRF1) were still detectable, and all others were not. This is indicated by a horizontal dCT line, which no longer correlates with CTs from Passage 2. OriP maps to 7,421–9,538, Qp to ~85,000 and EBNA-1 to ~96,000 (Fig. 2*c*). Hence, within the resolution of our analysis, these essential latent loci were selectively retained in HONE-1 clone 13 cells.

To independently confirm this observation, we applied unsupervised cluster analysis to the data (Fig. 4*d*). Again we found a dramatic difference between parental HONE-1 and HONE-1 clone 13 cells. The parental cell population lost the entire EBV genome at once, as indicated by the abrupt color change (yellow to blue) for almost all primers between p8 and p12. By contrast, HONE-1 clone 13 cells show a gradual loss of signal over time, corroborating the pair wise regression analyses (Figs. 4*a–4c*). Some genes were lost between p2 and p6. Others (middle section) were lost between p5 and p19. Signal fluctuation in between passages did occur. However, most of these fluctuations were within the margin of error and were only overemphasized in this particular representation, which is based on raw data rather than averages (Figs. 4*a–4c*). BWRF1, BYRF1 and BLRF3 signals were uniformly positive and therefore not used for comparison. These results confirm that HONE-1 clone 13 cells behave differently than the uncloned, parental HONE-1 population. The data suggests that HONE-1 clone 13 cells lose the viral episome by gradual fragmentation, resulting in defective episomes that retain the essential cis-elements longer than orfs with no known role in episome maintenance.

HONE-1 clone 13 cells lose the EBV episome through successive deletions and recombination

To explore further the scenario of accumulative deletion/recombination (Fig. 2*b*), we tested the hypothesis that adjacent orfs are retained or lost together during passage in culture. To do so, we established a statistical model based upon the relationship between orf map position and relative copy number of individual orfs for each passage. Using HONE-1 clone 13 cell Passages 2, 5, 10 and 19, we calculated the differences in signal (ddCT) between 1 orf and its immediate neighbor (+1), or its second (+2) and third (+3) adjacent orf as such: $ddCT(p_i) = dCT(p_{i+1}) - dCT(p_i)$, $ddCT(p_i) = dCT(p_{i+2}) - dCT(p_i)$, $ddCT(p_i) = dCT(p_{i+3}) - dCT(p_i)$. If 2 orfs within a given pair are present, signal difference $ddCT(p_i)$ is minimal for cells of the same passage number. If 1 orf within a given pair is lost then the signal difference $ddCT(p_i)$ is maximal. The further apart 2 orfs are, the more likely it is that a random recombination/deletion event removes 1 orf, but not the other. This is the principle of gene mapping by recombination frequency. By contrast, if the entire episome is only lost or maintained as a whole, then the signal difference $ddCT(p_i)$ between any 2 orfs will remain constant regardless of their relative location on the viral episome.

We computed Z scores of these $ddCT(p_i)$, which allowed us to evaluate relative orf retention at different passages independent of the total copy number. We established pairwise correlations for all possible combinations (data not shown). Except at Passage 19, where most of the orf signals were lost, significant overall correlations were evident, as even if individual orfs are lost by deletion, the majority of orfs remain linked to each other on the episome and therefore are present at similar levels. However, the further

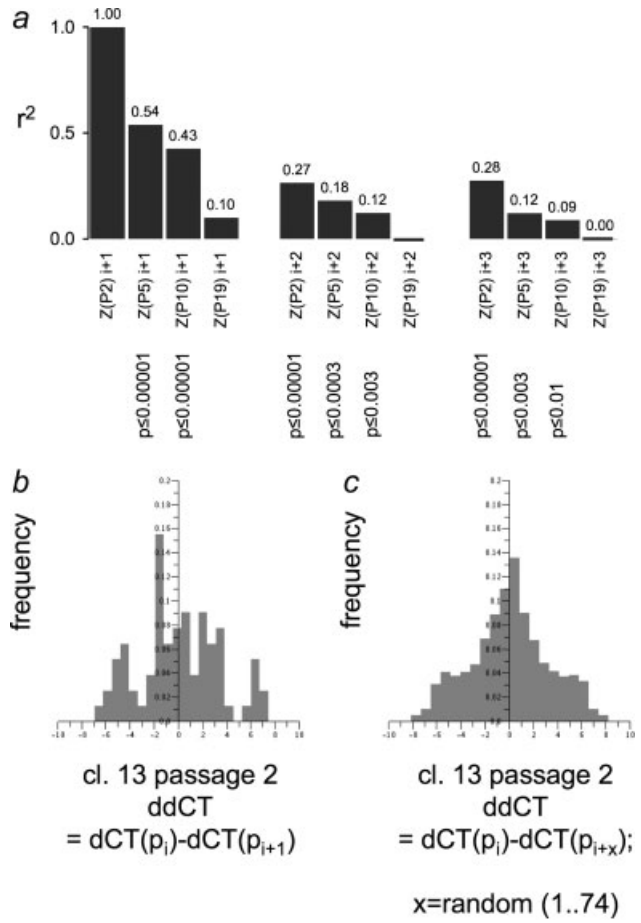

FIGURE 5 – Shown are statistical measures of the correlation in copy number between any 2 adjacent EBV orf at different passages. (*a*) Histogram of squared correlation coefficients (and *p* values) of the difference in levels (ddCT) between all orfs (as measured by our primer pairs) and their neighboring orfs. The first group represents the combinations of ddCT(i + 1), *i.e.*, between each orf and its nearest neighbor, at Passage 2 to all later passages (p6, p10, p19). The second group represents the correlations at Passage 2 to all later passages (p6, p10, p19) for the i + 2 neighbors and the third group for the i + 3 neighbors. More distant orfs are less correlated than adjacent orfs and levels for later passages are less correlated Passage 2 than earlier passages. Consistent with successive small deletions. (*b*) Shown is the observed distribution of relative differences between any 2 immediately adjacent orfs at passage p2, which is compared to a distribution (*c*) of random pairs of orfs (using 1,000 random combinations of the CT values).

apart (i + 1, 2, 3) any 2 orfs are located on the EBV episome, the less their relative levels correlate with each other (Fig. 5).

The squared Pearson correlation coefficients comparing Passage 2 (i + 1) standardized ddCTs to all other passages exemplify this approach (Fig. 5*a*). For the same input DNA, there exists a perfect correlation (r^2 = 1.00) of all primer pair distances to itself.

The i + 1 distances (immediately adjacent markers) were significantly correlated at Passage 5 (r^2 = 0.54) to Passage 2 and Passage 10 (r^2 = 0.43) to Passage 2, but not at Passage 19 (r^2 = 0.1), since at this point most of the episomes were lost. If viral episomes can only be lost as a whole, we would expect similar correlation coefficients for more distant markers (i + 2) and (i + 3) as well. This, however, was not the case.

There was less of a correlation when comparing i + 1 and i + 2 differences at Passage 2 (r^2 = 0.27), *i.e.*, for the same DNA than between different Passages 2 and 5 (r^2 = 0.54) for immediate neighbors (i + 1). Even less of a correlation was observed comparing i + 1 to i + 3 differences (rightmost group). This gradual decrease in correlation would not be expected if the entire episome were lost at the same time (Model A). This gradual decrease in correlations would also not be expected for completely random data as shown in Figures 5*b*–5*c*. Only a piecemeal loss of episomal genetic material is consistent with this result, which proves that more distantly located orfs are more likely to be separated by recombination or deletion.

The parental cells lost all orf signals at once and thus there were no significant correlations (data not shown). Hence, the HONE-1 clone 13 phenotype is unlikely to be due to a systematic bias, but reflects the underlying biological process of episomal loss.

Discussion

Episome maintenance and loss are fundamental to the persistence and oncogenesis of herpesviruses. Although episomal plasmid maintenance has been studied genetically in detail in bacteria and lower eukaryotes, (for example, the yeast 2-μm circle[30]) similar quantitative, genetic studies in human cells were limited by sensitivity issues before the use of PCR. Through our new technique of real-time QPCR-based microarrays, here, we are able to provide a detailed quantitative analysis of EBV episome loss in NPC.

The data presented here provide evidence for 2 consecutive and mechanistically distinct phases of EBV latent episome loss. As shown previously, the EBV episome is lost rapidly from as many as 25% of infected cells upon primary infection (reviewed in Ref. 31). It takes 2 to 3 weeks until an episome is stably established in the fraction of cells that can support long-term maintenance. During this first, "rapid-loss" phase the viral episome or artificial EBV oriP-dependent episomes are lost in their entirety. Afterward, the episome copy number remains constant. In EBV positive stable cell lines, the viral episome is replicated in synchrony with cellular replication and correctly partitioned at cell division in 97% of cells.[32] Three percent of cells even at this second "slow loss" stage lose the episome by a hitherto unspecified mechanism.[27] NPC offers a unique opportunity to study EBV episome loss because NPC-derived explant cultures lose the virus within 20 passages. In contrast, BL cell lines maintain EBV much longer, even though Akata and other BL cell lines lose the viral episome over time and accumulate defective episomes.[33,34] With the exception of HONE-1 clone 40 cells and C666-1 cells,[35] no NPC-derived cell line currently exists that stably carries an EBV genome.[9,12] The difference between NPC and BL has been attributed to the fact that BL cells and LCLs require some EBV transforming functions for growth in culture while NPC do not. This notion is corroborated by our observation that even though HONE-1 and clone 13 cells lose EBV, the EBV-negative cells continue to grow in culture (data not shown). Hence, BL and LCL cells, which lose the virus, die in culture leaving a 100% EBV-positive population to undergo the next cell division. Human NPC tumors and NPC xenografts retain EBV, presumably, because EBV is required for growth *in vivo*,[36] but it is unclear whether NPC cells require EBV for growth in culture.[37]

A reasonable concern is that we could potentially be observing outgrowth of a contaminating, EBV negative cell population such as HeLa cells. Such a scenario is inconsistent with our quantitative analysis (Figs. 4 and 5) showing the selective loss of some EBV genes, while retaining others ("slow loss phase"). Nevertheless, it is important to provide a history of the development of the HONE-1 parental, clone 40 and clone 13 cells. In the late 1980s, the Glaser laboratory (in collaboration with Dr. Kaitai Yao) prepared explant cultures from primary NPC biopsies. Detailed characterization of 2 such NPC cell lines derived from 2 separate biopsies (HNE-1 and HONE-1) were published.[11–13] A second NPC cell line (C666-1) containing a stable NPC genome has now been published.[35]

The HONE-1 parental cell population was established from one of the NPC biopsies and as uncloned cell populations were undoubtedly heterogenous for cell markers, karyotype and perhaps

for EBV-specific markers as well. As soon as the parental cell culture was established (Passages 2–3), we went through the process of preparing clone 13 and clone 40 cell lines using soft agar cloning. We focused initially on the HONE-1 clone 40 cells because these were EBV DNA positive and could be induced to produce virus by treating the cells with IUDR. As the clone 40 cells were being studied, the cells became contaminated with a slow-growing bacteria.[14]

Recently, we discovered a small number of uncontaminated frozen stocks of the initial, low-passage parental explant cultures and another clone, clone 13. These tested positive for EBV DNA by PCR (Fig. 1), and it is these cells that were used in this study. We have karyotyped these cells to exclude a possible contamination with other cells (Supplemental Fig. 1). On the one hand, it is disappointing that clone 13 does not stably maintain the EBV genome. On the other hand, the reproducible loss of the EBV episome from clone 13 and HONE-1 parental cultures provided the opportunity to quantitatively analyze episome loss in NPC.

Our biphasic model of EBV episome loss has 1 important limitation. It is population-based, since we used $\sim 10^6$ cells to derive DNA at each passage. The initial, "rapid loss phase" can be explained either as synchronous loss of excess episomes from every cell in the population each carrying the same EBV copy number, or as outgrowth of low episome carrying clones. The existence of clone 13, which starts out with a lower episome load, suggests that there is indeed variation in viral episome copy number within the initial NPC explant population. Perhaps one could even argue that a high EBV episome number is disadvantageous for growth in culture and hence cells with high episome loads are rapidly selected against. Further studies are needed to address this issue.

We set out to understand how the EBV episome is lost during the second "slow-loss phase". (*i*) Is the entire episome lost at once as episome-carrying cells are diluted out of the population and as epigenetic silencing of the viral genome[38] accumulates in the absence of selection? Or (*ii*) is the episome lost through successive deletion and recombination events until the essential cis-elements oriP, Qp and EBNA-1 are no longer within the same cell? Of note, as only a fraction of each population is used to seed the next flask, extremely variant cell clones and nonreplication competent pieces of EBV DNA are diluted out. Our study supports the second model by showing that different portions of the EBV episome were lost at different rates. Large deletions of the EBV episome occur naturally, and can yield stable episomes in BL. This is evidenced by the B95-8, which has lost $\sim$11 kbp in the LF3 region,[39] and the Daudi and P3HR-1 cell lines, which both have lost $\sim$8 kb in the EBNA2 region[40] and others.[33,41,42] Perhaps a particular variant virus confers a selective advantage to a particular clone, for instance by complementing a host gene defect.[43,44] Such a mechanism remains to be shown in the case of NPC and other EBV-associated epithelial cancers. That latent viral infection can confer a selective growth advantage is no doubt the case for EBV-infected lymphoma cells[45] as well as clones of endothelial cells infected with the related Kaposi's sarcoma-associated herpesvirus.[46]

We found that there exists a tissue-type-specific upper limit of the number episomes within a cell (Fig. 1). It appears to be lower in NPC than in BL. A similar observation holds true for Kaposi sarcoma-associated herpes virus (KSHV), where the average episome copy number in infected endothelial cell cultures is lower than in B lineage primary effusion lymphoma.[46,47] Upon initial explantation, most cells lose the entire episome rapidly and at once (Figs. 2 and 3). They are neither competent to maintain the viral episome nor did the EBV episome confer a selective advantage at this stage. However, in every generation individual clones exist, such as the HONE clone 13 in our study, which have the ability to maintain viral episomes after prolonged passage. We found that in these cells a second mechanism was responsible for the episome loss. Rather than losing all genes at once, successive deletions took place. We speculate that any viral episome will sustain deleterious mutations at the same rate as the cell's chromosome. Mutations that do not affect the essential latent replication and maintenance loci accumulate, because, less than 10% of viral genes are expressed during and required for latency. Only when one of the essential viral episome maintenance loci (EBNA-1, oriP and Qp) are hit is the entire episome lost. Based upon our array results shown in Figure 4, we propose that large deletions are rare, but small deletions and subsequent recombination events (size of 1 orf or smaller) occur more frequently.

EBV contains internal repeats in the BamW region, which may expand and contract during passage in culture. Our array contained no primers in the IR region, but 1 primer pair (BWRF1), which was able to anneal at multiple positions within BamW region (Fig. 3). It is therefore conceivable that contractions within the BamW region may affect calculations that involve this 1 BWRF1 primer pair. It would not affect the other 74 primer pairs or our statistical modeling. We did not see any anomalies in the CT values for BWRF1.

Using the novel approach presented here, the mechanism of episomal loss and selective marker retention can be analyzed for other latent, episomal viruses as well, such as for KSHV. Like EBV from NPC KSHV is lost upon explantation of primary Kaposi sarcoma biopsies in culture, such that to date not a single tumor-derived cell line exists that carries KSHV.[48,49] Yet, similar to long-term latent EBV persistence in BL, KSHV is indefinitely maintained in suspension cultures of PEL. Our approach is suitable for automation and high throughput analysis of clinical samples. It should be useful for the development of approaches to cure latent infection by accelerating the rate of viral episome loss.

Acknowledgements

We thank Lianbo Yu and Stanley Lemeshow in The Ohio State University Biostatistic Center for reviewing our statistical analyses, Luciana Leopold and Rolf Renne for critical reading. We thank Nyla Hereema, Director of the Ohio State University Comprehensive Cancer Center Cytogenetics Core Lab for the chromosome analysis.

References

1. Henle G, Henle W, Diehl V. Relation of Burkitt's tumor-associated herpes-ytpe virus to infectious mononucleosis. Proc Natl Acad Sci USA 1968;59:94–101.
2. Epstein MA, Achong BG, Barr YM. Virus particles in cultured lymphoblasts from Burkitt's lymphoma. Lancet 1964;15:702–3.
3. zur Hausen H, Schulte-Holthausen H, Klein G, Henle W, Henle G, Clifford P, Santesson L. EBV DNA in biopsies of Burkitt tumours and anaplastic carcinomas of the nasopharynx. Nature 1970;228: 1056–8.
4. Lupton S, Levine AJ. Mapping genetic elements of Epstein-Barr virus that facilitate extrachromosomal persistence of Epstein-Barr virus-derived plasmids in human cells. Mol cell biol 1985;5:2533–42.
5. Yates J, Warren N, Reisman D, Sugden B. A cis-acting element from the Epstein-Barr viral genome that permits stable replication of recombinant plasmids in latently infected cells. Proc Natl Acad Sci USA 1984;81:3806–10.
6. Yates JL, Warren N, Sugden B. Stable replication of plasmids derived from Epstein-Barr virus in various mammalian cells. Nature 1985; 313:812–5.
7. Tsai CN, Liu ST, Chang YS. Identification of a novel promoter located within the bam HI Q region of the Epstein-Barr virus genome for the EBNA 1 gene. DNA Cell Biol 1995;14:767–76.
8. Gu SU, Tann BF, Zeng Y, Zhou WP, Li KB, Zahao MC. Establishment of an epithelial cell line (CNE-2) from an NPC patient with poorly differenciated squamous cell carcinoma. Chin J Cancer 1983; 1:70–72.
9. Huang DP, Ho JH, Poon YF, Chew EC, Saw D, Lui M, Li CL, Mak LS, Lai SH, Lau WH. Establishment of a cell line (NPC/HK1) from a differentiated squamous carcinoma of the nasopharynx. Int J Cancer 1980;26:127–32.

10. Yoshiyama H, Imai S, Shimizu N, Takada K. Epstein-Barr virus infection of human gastric carcinoma cells: implication of the existence of a new virus receptor different from CD21. J Virol 1997;71: 5688–91.
11. Glaser R, Zhang HY, Yao KT, Zhu HC, Wang FX, Li GY, Wen DS, Li YP. Two epithelial tumor cell lines (HNE-1 and HONE-1) latently infected with Epstein-Barr virus that were derived from nasopharyngeal carcinomas. Proc Natl Acad Sci USA 1989;86:9524–8.
12. Yao KT, Zhang HY, Zhu HC, Wang FX, Li GY, Wen DS, Li YP, Tsai CH, Glaser R. Establishment and characterization of two epithelial tumor cell lines (HNE-1 and HONE-1) latently infected with Epstein-Barr virus and derived from nasopharyngeal carcinomas. Int J Cancer 1990;45:83–9.
13. Zhang HY, Yao K, Zhu HC, Glaser R. Expression of the Epstein-Barr virus genome in a nasopharyngeal carcinoma epithelial tumor cell line. Int J Cancer 1990;46:944–9.
14. Yang EV, Sood AK, Chen M, Li Y, Eubank TD, Marsh CB, Jewell S, Flavahan NA, Morrison C, Yeh PE, Lemeshow S, Glaser R. Norepinephrine up-regulates the expression of vascular endothelial growth factor, matrix metalloproteinase (MMP)-2, and MMP-9 in nasopharyngeal carcinoma tumor cells. Cancer Res 2006;66:10357–64.
15. Papin J, Vahrson W, Hines-Boykin R, Dittmer DP. Real-time quantitative PCR analysis of viral transcription. Methods Mol Biol 2004; 292:449–80.
16. Rice P, Longden I, Bleasby A. EMBOSS: the european molecular biology open software suite. Trends Genet 2000;16:276–7.
17. Rozen SaHJS. Primer3 Software Distribution. http://frodo.wi.mit.edu/primer3/primer3_code.html, 1998.
18. Kurokawa M, Ghosh SK, Ramos JC, Mian AM, Toomey NL, Cabral L, Whitby D, Barber GN, Dittmer DP, Harrington WJ, Jr. Azidothymidine inhibits NF-κB and induces Epstein-Barr virus gene expression in Burkitt lymphoma. Blood 2005;106:235–40.
19. Hilscher C, Vahrson W, Dittmer DP. Faster quantitative real-time PCR protocols may lose sensitivity and show increased variability. Nucleic Acids Res 2005;33:e182.
20. Papin J, Vahrson W, Hines-Boykin R, Dittmer DP. Real-time quantitative PCR analysis of viral transcription. Quantifying total viral gene transcription. In: Lieberman P, ed. Methods in molecular virology (DNA viruses). Humana Press, Totowa, NJ; 2004:449–80.
21. Dittmer DP. Transcription profile of Kaposi's sarcoma-associated herpesvirus in primary Kaposi's sarcoma lesions as determined by real-time PCR arrays. Cancer Res 2003;63:2010–15.
22. Cytogentic ISCoH. An international system for human cytogenetic nomenclature. Basel: Karger, 2005.
23. Seo Y, Stradmann-Bellinghausen B, Rittner C, Takahama K, Schneider PM. Sequence polymorphism of mitochondrial DNA control region in Japanese. Forensic Sci Int 1998;97:155–64.
24. Sato H, Takimoto T, Hatano M, Pagano JS, Raab-Traub N. Epstein-Barr virus with transforming and early antigen-inducing ability originating from nasopharyngeal carcinoma: mapping of the viral genome. J Gen Virol 1989;70:717–27.
25. Knox PG, Li QX, Rickinson AB, Young LS. In vitro production of stable Epstein-Barr virus-positive epithelial cell clones which resemble the virus:cell interaction observed in nasopharyngeal carcinoma. Virology 1996;215:40–50.
26. Bowtell D, Sambrook J. DNA microarrays: a molecular cloning manual. Cold Spring Harbor: Cold Spring Harbor Laboratory Press, 2003.
27. Leight ER, Sugden B. Establishment of an oriP replicon is dependent upon an infrequent, epigenetic event. Mol Cell Biol 2001;21:4149–61.
28. Yates JL, Guan N. Epstein-Barr virus-derived plasmids replicate only once per cell cycle and are not amplified after entry into cells. J Virol 1991;65:483–8.
29. Eisen MB, Spellman PT, Brown PO, Botstein D. Cluster analysis and display of genome-wide expression patterns. Proc Natl Acad Sci USA 1998;95:14863–8.
30. Broach J. The yeast 2μ circle. In: Strathern J, Jones E, Broach J, eds. The molecular biology of the yeast saccaromyces. Cold Spring Harbor: Cold Spring Harbor Laboratory Press, 1981:445–70.
31. Robertson ES. Epstein-Barr virus. Norfolk: Caister Academic Press, 2005.
32. Glaser R, Nonoyama M, Hampar B, Croce CM. Studies on the association of the Epstein-Barr virus genome and human chromosomes. J Cell Physiol 1978;96:319–25.
33. Kolman JL, Kolman CJ, Miller G. Marked variation in the size of genomic plasmids among members of a family of related Epstein-Barr viruses. Proc Natl Acad Sci USA 1992;89:7772–6.
34. Shimizu N, Yoshiyama H, Takada K. Clonal propagation of Epstein-Barr virus (EBV) recombinants in EBV-negative akata cells. J Virol 1996;70:7260–3.
35. Cheung ST, Huang DP, Hui AB, Lo KW, Ko CW, Tsang YS, Wong N, Whitney BM, Lee JC. Nasopharyngeal carcinoma cell line (C666–1) consistently harbouring Epstein-Barr virus. Int J Cancer 1999; 83:121–6.
36. Gilligan KJ, Rajadurai P, Lin JC, Busson P, Abdel-Hamid M, Prasad U, Tursz T, Raab-Traub N. Expression of the Epstein-Barr virus BamHI a fragment in nasopharyngeal carcinoma: evidence for a viral protein expressed in vivo. J Virol 1991;65:6252–9.
37. Tomei LD, Noyes I, Blocker D, Holliday J, Glaser R. Phorbol ester and Epstein-Barr virus dependent transformation of normal primary human skin epithelial cells. Nature 1987;329:73–5.
38. Chau CM, Lieberman PM. Dynamic chromatin boundaries delineate a latency control region of Epstein-Barr virus. J Virol 2004;78:12308–19.
39. Bankier AT, Deininger PL, Farrell PJ, Barrell BG. Sequence analysis of the 17,166 base-pair EcoRI fragment C of B95–8 Epstein-Barr virus. Mol Biol Med 1983;1:21–45.
40. Jones MD, Foster L, Sheedy T, Griffin BE. The EB virus genome in Daudi Burkitt's lymphoma cells has a deletion similar to that observed in a non-transforming strain (P3HR-1) of the virus. Embo J 1984;3:813–21.
41. Razzouk BI, Srinivas S, Sample CE, Singh V, Sixbey JW. Epstein-Barr virus DNA recombination and loss in sporadic Burkitt's lymphoma. J Infect Dis 1996;173:529–35.
42. Srinivas SK, Sample JT, Sixbey JW. Spontaneous loss of viral episomes accompanying Epstein-Barr virus reactivation in a Burkitt's lymphoma cell line. J Infect Dis 1998;177:1705–9.
43. Kelly GL, Milner AE, Baldwin GS, Bell AI, Rickinson AB. Three restricted forms of Epstein-Barr virus latency counteracting apoptosis in c-myc-expressing Burkitt lymphoma cells. Proc Natl Acad Sci USA 2006;103:14935–40.
44. Kelly GL, Milner AE, Tierney RJ, Croom-Carter DS, Altmann M, Hammerschmidt W, Bell AI, Rickinson AB. Epstein-Barr virus nuclear antigen 2 (EBNA2) gene deletion is consistently linked with EBNA3A, -3B, and -3C expression in Burkitt's lymphoma cells and with increased resistance to apoptosis. J Virol 2005;79:10709–17.
45. Ruf IK, Rhyne PW, Yang H, Borza CM, Hutt-Fletcher LM, Cleveland JL, Sample JT. Epstein-Barr virus regulates c-MYC, apoptosis, and tumorigenicity in Burkitt lymphoma. Mol Cell Biol 1999;19:1651–60.
46. An FQ, Folarin HM, Compitello N, Roth J, Gerson SL, McCrae KR, Fakhari FD, Dittmer DP, Renne R. Long-term-infected telomerase-immortalized endothelial cells: a model for Kaposi's sarcoma-associated herpesvirus latency in vitro and in vivo. J Virol 2006;80:4833–46.
47. Renne R, Lagunoff M, Zhong W, Ganem D. The size and conformation of Kaposi's sarcoma-associated herpesvirus (human herpesvirus 8) DNA in infected cells and virions. J Virol 1996;70:8151–4.
48. Herndier BG, Werner A, Arnstein P, Abbey NW, Demartis F, Cohen RL, Shuman MA, Levy JA. Characterization of a human Kaposi's sarcoma cell line that induces angiogenic tumors in animals. AIDS 1994;8:575–81.
49. Grundhoff A, Ganem D. Inefficient establishment of KSHV latency suggests an additional role for continued lytic replication in Kaposi sarcoma pathogenesis. J Clin Invest 2004;113:124–36.